Talanta 111 (2013) 178–182

Contents lists available at SciVerse ScienceDirect

Talanta

journal homepage: www.elsevier.com/locate/talanta

Microfluidic cytometer based on dual photodiode detection for cell size and deformability analysis

Qin-Qin Ji [a,1,2], Guan-Sheng Du [a,b,1], Martijn J. van Uden [b,3], Qun Fang [a,*], Jaap M.J. den Toonder [b,c,**]

[a] Institute of Microanalytical Systems, Department of Chemistry, Zhejiang University, Hangzhou 310058, China
[b] Materials Technology Institute, Eindhoven University of Technology, Eindhoven 5600MB, The Netherlands
[c] Philips Research, Eindhoven 5656AE, The Netherlands

ARTICLE INFO

Article history:
Received 18 February 2013
Accepted 1 March 2013
Available online 13 March 2013

Keywords:
Microfluidic cytometer
Cell deformability
Cell size
Dual photodiodes

ABSTRACT

Cellular mechanical properties play an important role in disease diagnosis. Distinguishing cells based on their mechanical properties provides a potential method for label-free diagnosis. In this work, a convenient and low-cost microfluidic cytometer was developed to study cell mechanical properties and cell size based on the change of transmission intensity, using a low-cost commercial laser as a light source and two photodiodes as detectors. The cells pass through a narrow microchannel with a width smaller than the cell dimension, integrated in a polydimethylsiloxane chip, below which the laser is focused. The transit time of individual cells is measured by the time difference detected by two photodiodes. This device was used to study the difference in cell mechanical properties between HL60 cells treated with and without Cytochalasin D. Furthermore, it was also applied to distinguish cells with different diameters, HL60 cells and red blood cells, by measuring the transmission intensity.

1. Introduction

Cell mechanical properties play an important role in a number of processes, such as cell migration, invasion, division, and signaling. These mechanical properties are dynamically governed by the cytoskeleton, whose structure can be changed by the development of several diseases, such as malaria [1,2], cancer [2–4], and glaucoma [5]. A variety of techniques have been developed to measure cell mechanical properties, including micropipette aspiration [6,7], filtration [8], atomic force microscopy (AFM) [9–11], microplate stretching [12] and magnetic tweezers [13]. Although these methods can be used to assess cell mechanical properties, further application is limited due to their complex structure, low-throughput analysis and labor intensity.

Some microfluidic devices provide a possible approach to detect cell mechanical properties by using low quantities of samples and reagents in a controlled microenvironment on a simplified platform [14–20]. These devices usually require optical imaging of the cells to detect the cell mechanical properties, e.g. using a charge-couple device (CCD) camera. An array of elastomeric microposts was fabricated to characterize the subcellular distribution of mechanical properties by studying deflection images of multiple posts which were attached by a single cell [15–17]. Multilayer devices were also used to study cell viscoelastic properties by measuring area of recovery snapshots of cells after their deformation [19]. However, the throughputs of these approaches for cell analysis are usually quite low (<1 cell min^{-1}).

Several other microfluidic cytometer systems were developed to achieve high-throughput analysis of biomechanical properties of cells, such as deformability [21–32]. In these systems, a high-speed camera is usually utilized to capture the images of cells that are forced to deform inside the devices. These images are further analyzed to extract cell shape information and correlate it with cell mechanical properties. Bao et al. reported electroporation-induced cell deformation in a microfluidic device as a biomarker to differentiate cancer cells from normal ones for their higher degree of swelling [22]. Guck et al. distinguished human erythrocytes from mouse fibroblasts by comparing their difference in viscoelastic properties when micromanipulated by optical stretchers. Different indexes were developed to evaluate the viscoelatic properties of cells, for example, the ratio of the major to minor axes of the deforming cells [23,24]. Shelby et al. used a narrow channel to deform plasmodium falciparum-infected erythrocytes and normal erythrocytes by videos recording cell recovery and

* Correspondence to: Institute of Microanalytical Systems, Chemistry Experiment Building, Room 101, Zhejiang University (Zijingang Campus), Hangzhou 310058, PR China. Tel.: +86 571 88206771; fax: +86 571 88273572.
** Corresponding author at: Philips Research, High Tech Campus 34, 5656 AE Eindhoven, and Eindhoven University of Technology, Postbox 513, 5600 MB Eindhoven, The Netherlands. Tel.: +31 6 44146639.
E-mail addresses: fangqun@zju.edu.cn, fangqun101@gmail.com (Q. Fang), jaap.den.toonder@philips.com (J.M.J. den Toonder).
[1] The first two authors contributed equally to this work.
[2] Current address: Department of Chemistry, Brown University, Providence, 02912, USA.
[3] Current address: Philips Lighting, Eindhoven, 5611 BD, The Netherlands.

0039-9140/$ - see front matter © 2013 Elsevier B.V. All rights reserved.
http://dx.doi.org/10.1016/j.talanta.2013.03.004

rupture when squeezed by the narrow channel [25]. Rosenbluth et al. used a bifurcating microchannel network to investigate transit time of red blood cells and neutrophils passing through. The transit time could be quantified automatically from images recorded by a CCD camera and analyzed by home-made software [26]. Chen et al. coupled a high-speed camera with electric field generated by electrodes integrated in a microfluidic channel to obtain both elongational properties and impedance profiles of cells [27]. Abkarian et al. studied dynamics and hemorheology of single and multiple red blood cells and white blood cells by a similar design of microchannel [28]. However, the applications of these methods are limited by their relatively high cost of implementation and complex design. In addition, the post-image-analysis process makes it difficult to provide a real-time result.

In this article, an integrated and low-cost microfluidic cytometer was developed to probe cell mechanical properties and cell size based on simple dual photodiode detection. The transit times and transmission light intensities of cells when they pass through a narrow microchannel on a microchip were measured by using two photodiodes to capture the variation of the transmission intensity of a laser beam focused within the channel detection region. The present system was applied in the study of the difference in cell mechanical properties between HL60 cells and HL60 cells treated by Cytochalasin D (CytoD). Furthermore, cells with different diameters (HL60 cells and red blood cells) were also studied using this approach.

2. Experimental section

2.1. Chemicals and materials

All solvents and chemicals used were of reagent grade unless otherwise stated. Deionized water was used throughout. A silicon mold was provided by Philips Research (Eindhoven, the Netherlands). Phosphate buffered saline (PBS), fetal bovine serum (FBS), and Roswell Park Memorial Institute (RPMI) 1640 medium with 1% l-glutamine, 5% penicillin/streptomycin were obtained from Genom Biological Medicine Co. (Hangzhou, China). Complete culture medium was RPMI 1640 medium supplemented with 10% FBS. Bovine serum albumin (BSA) was obtained from Shenggong Bioengineering Co. (Shanghai, China). Polydimethylsiloxane (PDMS) prepolymer and cross-linker were obtained from Dow Corning (Sylgard 184, Midland, USA). CytoD was obtained from Sigma-Aldrich (St. Louis, USA).

2.2. System setup

A PDMS chip with microchannel configuration (as shown in Fig. 1) was fabricated using a soft lithography approach [33]. A PDMS substrate was cast at 80 °C for 1 h with a mixing ratio of 10:1 for PDMS prepolymer and cross-linker on the silicon mold structured by photolithography and deep reactive ion etching (DRIE) techniques. The solidified PDMS substrate was peeled off from the silicon mold, and bonded with another PDMS substrate after exposure to oxygen plasma for about 50 s. Two types of chip were fabricated. One chip had a 6-μm-wide, 200-μm-long, and 9.6-μm-high narrow channel for cell deformability analysis, and another chip had a narrow channel with a width of 12 μm, a height of 9.6 μm and a length of 250 μm for cell size analysis. The channel inlet end was cut into a cone shape to serve as a sampling probe. Then the PDMS chip was placed on a microscope slide with its sampling probe extending out. The outlet of the channel was connected with a waste reservoir via a Tygon tubing to provide the driving force for cells. A slotted-vial array (SVA) system was used to sequentially introduce buffer solution and different cell suspensions into the chip channel. The SVA system was made as previously described elsewhere [34,35]. The system setup is shown in Fig. 1. For cell detection, a red beam from a laser diode (AD6320 PFG, 10 mW, A-Laser Technology Co., Guangzhou, China) was focused below the center of the channel through an objective lens (×25, Mic Opto-electronics Technology Co., Shenzhen, China). Two photodiodes (OPT301, Texas Instrument Co., Texas, USA) were fixed 28 cm above the chip with a mutual distance of 5 cm to detect the transmission intensity variations when the cells pass through the narrow channel. An inverted microscope coupled with a CCD camera (UMD200, Superimage Digital Technology Exploitation Co., Hangzhou, China) was used to observe cells in the channel, as well as the laser's focal point before experiments.

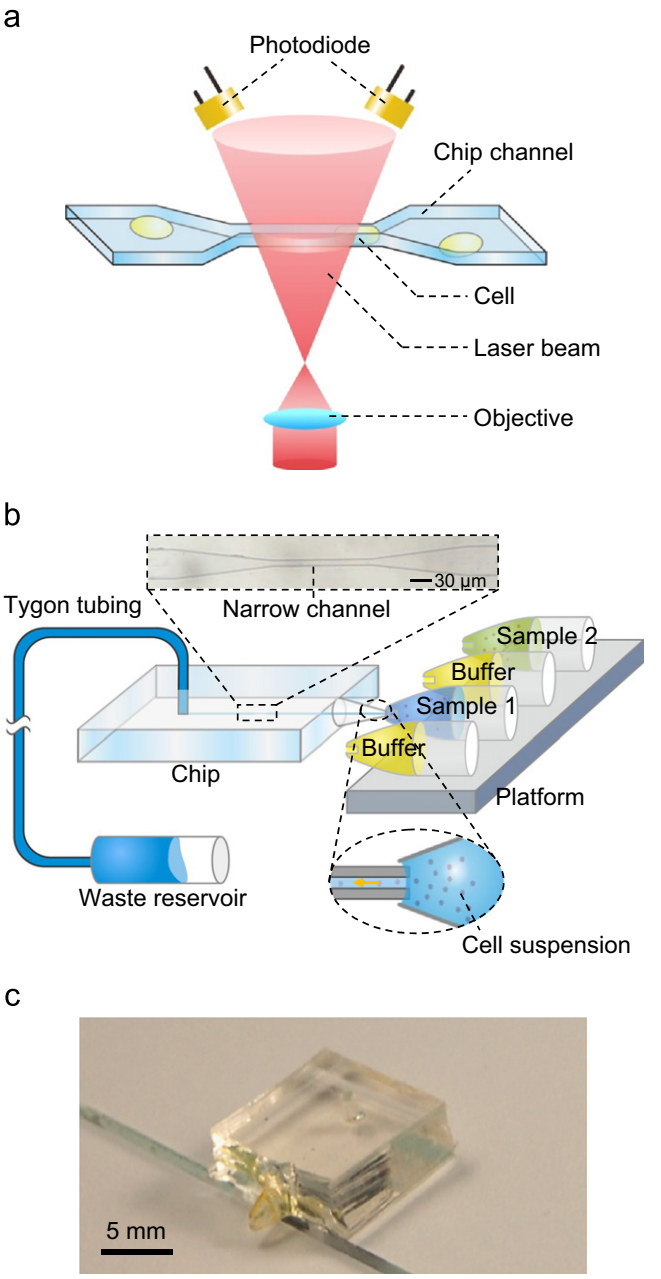

Fig. 1. Schematic diagrams of the setup (a) and the optical detection module (b) of the microfluidic cytometer (not to scale), and (c) the photograph of the PDMS chip.

2.3. Cell culture

Human promyelocytic leukemia cells (HL60 cells) were obtained from the Cell Bank of the Chinese Academy of Science (Shanghai, China). The cells were grown in complete RPMI culture medium, maintained in a 5% CO_2, 95% humidified atmosphere at 37 °C with cell density kept from 10^5 to 10^6 cells/mL. The RPMI culture medium was refreshed every 2–3 days. Before use, red blood cells (RBC) were collected from a healthy adult female volunteer aged 24 after obtaining her permission. Both of the cells were diluted to an optimized, relatively low concentration around 1×10^5 cell/mL with complete culture medium before experiments —at this concentration, clogging of the device by the cells or the possibility of two or more cells entering the narrow channel at the same time could be mostly avoided.

In the experiments of Section 3.3, the HL60 cells were pretreated by adding 2 μM CytoD in the complete culture medium for 1 h to disrupt actin structures in the cells. After that, the cells were centrifuged and re-suspended by PBS.

2.4. Procedures

Before the actual experiment, the chip channel was flushed with 20 mg/mL BSA solution for 20 min to eliminate non-specific cell adhesion to the surface of channel. The slotted vials were filled with cell suspensions and PBS. The driving force for fluids in the channel was provided by the pressure from an adjustable difference in liquid levels between the PDMS chip and the waste reservoir. Hence the cell suspension was introduced into and flown through the chip channel by a constant pressure produced by the liquid level difference between the PDMS chip and the waste reservoir. Transmission intensity was measured by the two photodiodes via a data acquisition card with 5000 Hz (USB-6008, National Instruments, Austin, USA). Between two cell samples, the chip channel was flushed with PBS to wash away any remaining cells from the previous measurement.

2.5. Data analysis

A typical transmission intensity recording in an HL60 cell experiment is shown in Fig. 2. Two negative peaks were recorded for each individual cell by the prior and posterior photodiodes. The negative peak corresponding to a decrease of transmission intensity was caused by the reflection and scattering of the detection light beam by the cell. A home-made MATLAB program (http://www.billauer.co.il/peakdet.html) was used to detect the negative peaks. The transit time of cell passing through the detection region in the channel, which is related to cell deformability, was measured by calculating the time difference between the negative peak pair (N2–N1). The data was smoothed by averaging using a window of 50 points.

3. Results and discussion

3.1. System design

In many of the previously reported microfluidic cytometer systems, cells are detected using highly sensitive photomultiplier tubes or high-speed CCD imaging chips [36–38]. In this work, to simplify the system and reduce system expense, one laser light source and two low-cost photodiodes were used instead. The transmission intensity was measured by locating the laser focal point below the narrow channel as illustrated in Fig. 1. A narrow channel design was used to induce cell deformation when cells pass through the channel and achieve distinguishing of cell

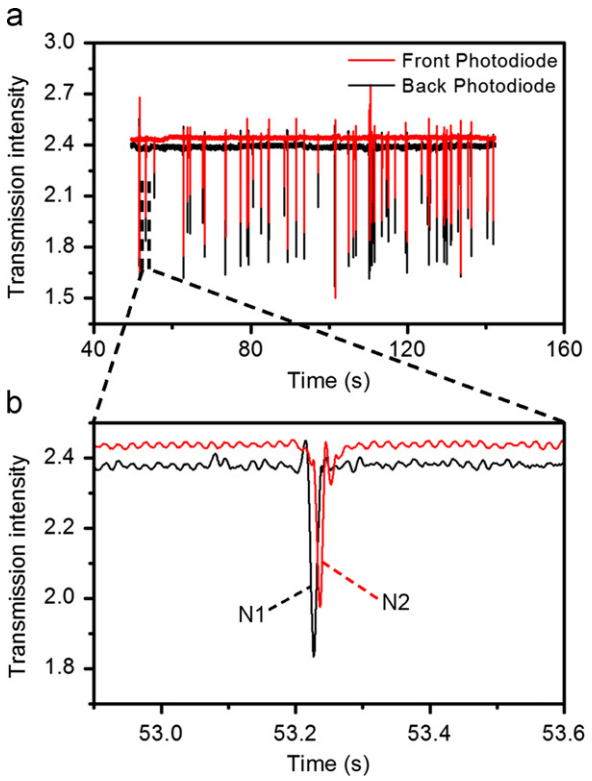

Fig. 2. Typical recordings of transmission intensity in a cell experiment. (a) Signals generated by a number of HL60 cells passing through the narrow channel. (b) Typical signals detected by two photodiodes of one HL60 cell in (a).

deformability [25–27,30–32]. We investigated the effect of the position of laser focal point from 500 μm below to 300 μm above the narrow channel on the cytometer performance using a PDMS chip with 6-μm-wide and 200-μm-long narrow channel. Typical recordings for HL60 cells with an average diameter of about 10 μm are as shown in Fig. 3. The transit time obtained from the negative peak pair was mainly determined by two obvious parameters, namely the speed of the cell passing through the detection region and the length of detection region. On one hand, the cell deformability and the driving force affected the speed of the cell passing through the detection region. Larger driving force increases the passing speed of cells. The cell deformability was changed when treating the cells by drugs (i.e. CytoD). On the other hand, the length of the detection region was influenced by the relative position of laser focal point to the chip channel. When the laser beam was focused inside the channel, the two negative peaks were entirely overlapping as the two photodiodes measured the light beam from the same position (Fig. 3f). The detection region was enlarged when the laser focusing point was located away from the chip channel. The larger the region of the laser beam covered, the longer the cell transit time could be measured, which increases the accuracy of measurement. However, with the laser beam focused away from the channel too far, the beam covers a larger channel region, and the probability of two consecutive cells passing through the channel interfering with the time measurement also increases. Compromising between the accuracy and interference between adjacent cells, we chose the position of laser focusing point at 400 μm below the chip channel.

3.2. Position of the waste reservoir

In most of the previous microfluidic cytometers for study of cell mechanical properties, the measurements for cell deformation were carried out under constant flow rate mode using syringe

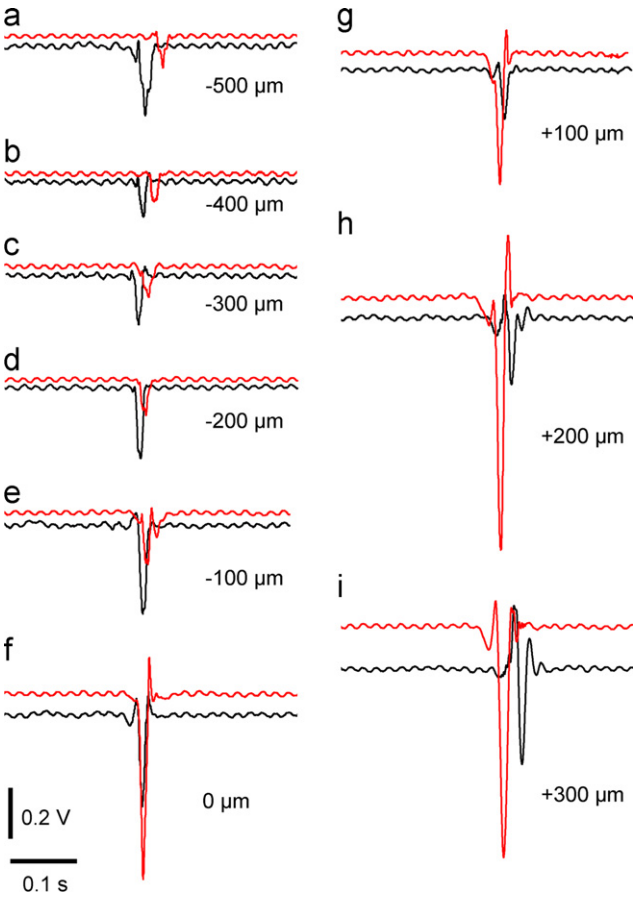

Fig. 3. Typical signals obtained by the two photodiodes when one HL60 passing through the narrow channel with different distances between the laser focal point and the chip channel of (a) −500 μm, (b) −400 μm, (c) −300 μm, (d) −200 μm, (e) −100 μm, (f) 0 μm, (g) +100 μm, (h) +200 μm and (i) +300 μm.

pumps [25,26,39]. In the present system, the measurement of cell deformation was performed by measuring the transit time for a cell passing through the narrow channel. In such a system, the constant flow rate mode would produce difference change of pressure applied to each cell when passing through the narrow channel since the presence of the cell changes the effective resistance of the system, which may affect the consistency of measured transit time [40]. Therefore, a constant pressure mode was employed in the present system. We used a Tygon tubing to connect the chip channel with the horizontal waste reservoir, and generate a liquid-level difference between them to provide a constant driving pressure for cell suspension. A similar method was used in a high-throughput microchip-based flow-injection analysis system [34].

We tested the effect of the liquid-level difference between the chip channel and waste reservoir using HL60 cells as a model sample. The histograms of normal distributions of the cell transit time with the change of liquid-level difference were determined, and the results are as shown in Fig. 4. The peak value of the transit time at liquid-level difference of 10 cm, 15 cm and 20 cm was 72.4 ms, 35.5 ms, and 26.6 ms, respectively. A spread in transit times is observed for each liquid-level difference, and can be attributed to the spread in cell size. For a larger liquid-level difference, the distribution of the transit time showed more spread; thus the difference of cell transit times could be better identified. However, we observed that the probability of cell blocking the narrow channel also increased with the decrease of the liquid-level difference. Therefore, a liquid-level difference of 15 cm between the chip channel and waste reservoir was employed in the present system,

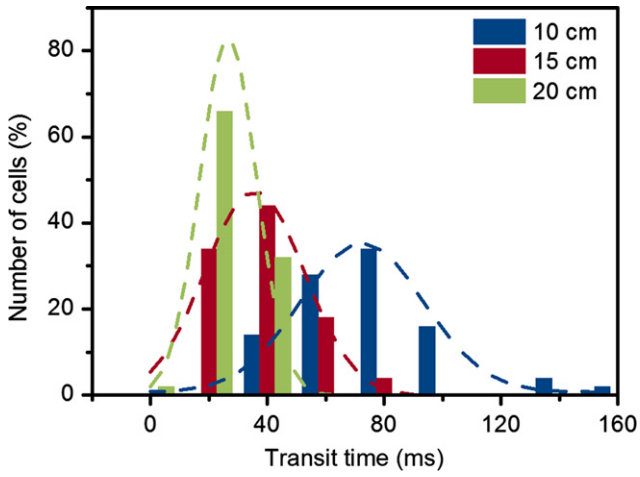

Fig. 4. Histogram of the transit time of HL60 cells at different liquid-level differences of 10 cm, 15 cm and 20 cm, obtained from ~50 cells for each condition.

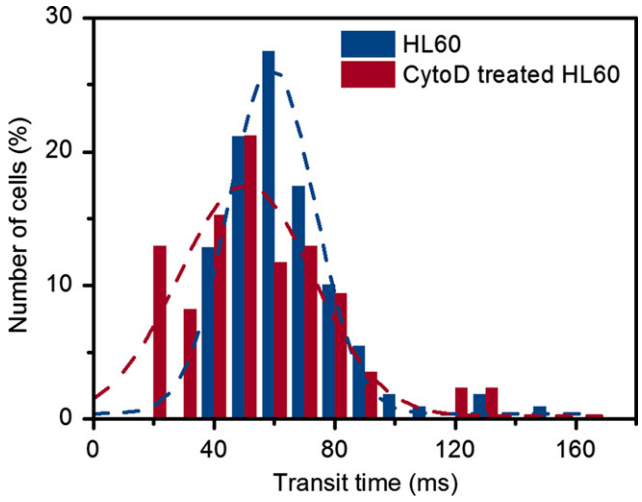

Fig. 5. Histograms of the transit times of HL60 cells (blue bars) and CytoD treated HL60 cells (red bars). Each histogram includes data from ~100 cells. (For interpretation of the references to color in this figure legend, the reader is referred to the web version of this article.)

corresponding to an estimated pressure for cell sample introduction of 1470 Pa. The flow rate inside the channel, measured using the video recorded by the CCD camera when cells passed through the microchannel, was 2 mm s^{-1}.

3.3. Performance of the cytometer

CytoD is known to be an agent that degrades the actin network in the cytoskeleton, so that the cell's elastic modulus reduces while maintaining the cell shape [41]. To evaluate the performance of the cytometer in distinguishing cell mechanical properties, the transit times of HL60 cells treated with and without CytoD were determined. A typical throughput of 33 cells min^{-1} in the cytometer was obtained (Fig. 2). As shown in Fig. 5, an obvious left shift of cell transit time distribution is observed when HL60 cells are treated by 2 μm CytoD. The cell sample for each group consists of more than 100 cells. In the transit times distribution of the treated cells, shifted toward shorter transit time, more than 20% of the cells have a transit time of less than 35 ms. The maximum peak of transit time distribution appears around 55 ms. The transit times of normal HL60 cells show a Gaussian distribution and the

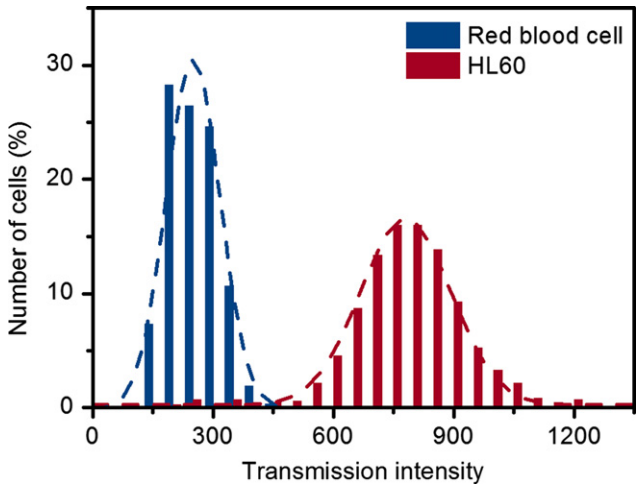

Fig. 6. Histograms of the transmission intensity distribution of HL60 cells (blue bars) and RBC (red bars). Each histogram contains data from ~600 cells. (For interpretation of the references to color in this figure legend, the reader is referred to the web version of this article.)

maximum peak is around 65 ms. This indicates that the present system can probe the variation of the elastic modulus of cells by measuring the transit time variation.

To distinguish between cells with clearly different sizes, the height of negative peaks caused by the cells passing through the microchannel was measured. Fig. 6 shows results for HL60 cells and RBC—these two types of cells have different mechanical properties, but their main distinguishing feature is their difference in cells sizes, i.e. 10 μm for HL60 cells and 5 μm for RBC. The transmission intensity significantly changes when cells with different size pass through a narrow channel with a width of 12 μm and a length of 250 μm. As shown in Fig. 6, there is significant difference between the transmission intensity distribution of RBC and HL60 cells. The transmission intensities of more than 90% of RBC are around 300 mV. However, under the same experimental condition, the transmission intensity distribution of HL60 cells is mainly around 800 mV.

4. Conclusion

We developed a microfluidic cytometer with a micro-channel to study cellular mechanical properties and distinguish between cells with different sizes, based on a simple and low cost optical setup consisting of a low-cost laser and two basic photodiodes for detection. On the basis of the optical structure, a portable cytometer can be developed, which may eventually find application in miniaturized instruments for home-use.

Although the throughput of the system is lower than those of commercial cytometers, it could be applied in screening of some diseases that are known to affect cell mechanical properties or cell size. The throughput of the present system is expected to be improved by using a more sensitive data acquisition card and photodiodes, or using multi-channel microchips.

Acknowledgments

Financial supports from National Natural Science Foundation of China (Grant nos. 20775071, 20825517 and 20890020), Ministry of Science and Technology of China (Grant nos. 2007CB714503 and 2007CB914100), and the Brain-bridge Project from Philips Research are gratefully acknowledged.

References

[1] F.K. Glenister, R.L. Coppel, A.F. Cowman, N. Mohandas, B.M. Cooke, Blood 99 (2002) 1060–1063.
[2] S. Suresh, J. Spatz, J.P. Mills, A. Micoulet, M. Dao, C.T. Lim, M. Beil, T. Seufferlein, Acta Biomater. 1 (2005) 15–30.
[3] M. Lekka, P. Laidler, D. Gil, J. Lekki, Z. Stachura, A.Z. Hrynkiewicz, Eur. Biophys. J. 28 (1999) 312–316.
[4] S. Suresh, Acta. Biomater. 3 (2007) 413–438.
[5] D.E. Ingber, Ann. Med. 35 (2003) 564–577.
[6] E. Evans, A. Yeung, Biophys. J. 56 (1989) 151–160.
[7] R.M. Hochmuth, J. Biomech. 33 (2000) 15–22.
[8] S.C. Gifford, M.G. Frank, J. Derganc, C. Gabel, R.H. Austin, T. Yoshida M.W. Bitensky, Biophys. J. 84 (2003) 623–633.
[9] C. Rotsch, M. Radmacher, Biophys. J. 78 (2000) 520–535.
[10] M.J. Rosenbluth, W.A. Lam, D.A. Fletcher, Biophys. J. 90 (2006) 2994–3003.
[11] C. Rotsch, K. Jacobson, M. Radmacher, Proc. Natl. Acad. Sci. USA 96 (1999) 921–926.
[12] O. Thoumine, A. Ott, J. Cell Sci. 110 (1997) 2109–2116.
[13] A.R. Bausch, W. Moller, E. Sackmann, Biophys. J. 76 (1999) 573–579.
[14] W.L. Ong, K.C. Tang, A. Agarwal, R. Nagarajan, L.W. Luo, L. Yobas, Lab Chip 7 (2007) 1357–1366.
[15] N.Q. Balaban, U.S. Schwarz, D. Riveline, P. Goichberg, G. Tzur, I. Sabanay, D. Mahalu, S. Safran, A. Bershadsky, L. Addadi, B. Geiger, Nat. Cell Biol. 3 (2001) 466–472.
[16] J.L. Tan, J. Tien, D.M. Pirone, D.S. Gray, K. Bhadriraju, C.S. Chen, Proc. Natl. Acad. Sci. USA 100 (2003) 1484–1489.
[17] N.J. Sniadecki, A. Anguelouch, M.T. Yang, C.M. Lamb, Z. Liu, S.B. Kirschner, Y. Liu, D.H. Reich, C.S. Chen, Proc. Natl. Acad. Sci. USA 104 (2007) 14553–14558.
[18] D.N. Hohne, J.G. Younger, M.J. Solomon, Langmuir 25 (2009) 7743–7751.
[19] G. Du, A. Ravetto, Q. Fang, J.M.J. den Toonder, Biomed. Microdevices 13 (2011) 29–40.
[20] C.H. Hsu, C. Chen, A. Folch, Lab Chip 4 (2004) 420–424.
[21] K. Tsukada, E. Sekizuka, C. Oshio, H. Minamitani, Microvasc. Res. 61 (2001) 231–239.
[22] N. Bao, Y. Zhan, C. Lu, Anal. Chem. 80 (2008) 7714–7719.
[23] J. Guck, R. Ananthakrishnan, H. Mahmood, T.J. Moon, C.C. Cunningham, J. Kas, Biophys. J. 81 (2001) 767–784.
[24] J. Guck, S. Schinkinger, B. Lincoln, F. Wottawah, S. Ebert, M. Romeyke, D. Lenz, H.M. Erickson, R. Ananthakrishnan, D. Mitchell, J. Kas, S. Ulvick, C. Bilby, Biophys. J. 88 (2005) 3689–3698.
[25] J.P. Shelby, J. White, K. Ganesan, P.K. Rathod, D.T. Chiu, Proc. Natl. Acad. Sci. USA 100 (2003) 14618–14622.
[26] M.J. Rosenbluth, W.A. Lam, D.A. Fletcher, Lab Chip 8 (2008) 1062–1070.
[27] J. Chen, Y. Zheng, Q. Tan, E. Shojaei-Baghini, Y.L. Zhang, J. Li, P. Prasad, L. You X.Y. Wu, Y. Sun, Lab Chip 11 (2011) 3174–3181.
[28] M. Abkarian, M. Faivre, H.A. Stone, Proc. Natl. Acad. Sci. USA 103 (2006) 538–542.
[29] D.R. Gossett, H.T.K. Tse, S.A. Lee, Y. Ying, A.G. Lindgren, O.O. Yang, J.Y. Rao A.T. Clark, D. Di Carlo, Proc. Natl. Acad. Sci. USA 109 (2012) 7630–7635.
[30] W.G. Lee, H. Bang, H. Yun, J. Lee, J. Park, J.K. Kim, S. Chung, K. Cho, C. Chung D.C. Han, J.K. Chang, Lab Chip 7 (2007) 516–519.
[31] A. Adamo, A. Sharei, L. Adamo, B. Lee, S. Mao, K.F. Jensen, Anal. Chem. 84 (2012) 6438–6443.
[32] H.W. Hou, Q.S. Li, G.Y.H. Lee, A.P. Kumar, C.N. Ong, C.T. Lim, Biomed. Microdevices 11 (2009) 557–564.
[33] M.A. Unger, H.P. Chou, T. Thorsen, A. Scherer, S.R. Quake, Science 288 (2000) 113–116.
[34] W.B. Du, Q. Fang, Q.H. He, Z.L. Fang, Anal. Chem. 77 (2005) 1330–1337.
[35] W.B. Du, Q. Fang, Z.L. Fang, Anal. Chem. 78 (2006) 6404–6410.
[36] M.A. McClain, C.T. Culbertson, S.C. Jacobson, J.M. Ramsey, Anal. Chem. 73 (2001) 5334–5338.
[37] Z. Wang, J. El-Ali, M. Engelund, T. Gotsaed, I.R. Perch-Nielsen, K.B. Mogensen, D. Snakenborg, J.P. Kutter, A. Wolff, Lab Chip 4 (2004) 372–377.
[38] N. Pamme, R. Koyama, A. Manz, Lab Chip 3 (2003) 187–192.
[39] M. Kim, D.J. Hwang, H. Jeon, K. Hiromatsu, C.P. Grigoropoulos, Lab Chip 9 (2009) 311–318.
[40] D.J. Beebe, G.A. Mensing, G.M. Walker, Annu. Rev. Biomed. Eng. 4 (2002) 261–286.
[41] D.W. Goddette, C. Frieden, J. Biol. Chem. 261 (1986) 5974–5980.